Journal of Microscopy, Vol. 233, Pt 2 2009, pp. 244–250
Received 8 April 2008; accepted 13 August 2008

Chemically specific imaging of cryptosporidium oocysts using coherent anti-Stokes Raman scattering (CARS) microscopy

S. MURUGKAR*, C.L. EVANS†,‡, X.S. XIE† & H. ANIS*
**School of Information Technology and Engineering (SITE), University of Ottawa, 800 King Edward, P.O. Box 450, Stn A, Ottawa, Ontario K1N 6N5, Canada*
†Department of Chemistry and Chemical Biology, Harvard University, 12 Oxford St, Cambridge, Massachusetts 02138, U.S.A.

Key words. Coherent anti-Stokes Raman scattering, cryptosporidium oocyst, microscopy.

Summary

We demonstrate the application of coherent anti-Stokes Raman scattering microscopy for the rapid, label-free chemical imaging of waterborne pathogens. Chemically selective images of cryptosporidium were acquired in just a few seconds using coherent anti-Stokes Raman scattering microscopy, demonstrating its capability for the rapid detection of cryptosporidium at the single oocyst level. We discuss the applicability of such a technique in a near-real time automated water testing system.

Introduction

Many of the infectious diseases that are the largest source of human mortality in the world are waterborne and have tremendous adverse impacts in developing countries. Although developed countries have been more successful in controlling waterborne pathogens, water quality problems are still prevalent (Edge *et al.*, 2003). Waterborne pathogens such as bacteria, protozoa and viruses can pose significant human health threats as exemplified by the tragedy in Walkerton, Ontario, Canada, in the year 2000 where seven people died and 2500 became ill due to the contamination of the town's water supply by a deadly strain of the *Escherichia coli* bacteria. A drinking water incident in 1993 related to Cryptosporidiosis in Milwaukee, Wisconsin, U.S.A. resulted in 54 deaths and over 400 000 cases of illness (Edge *et al.*, 2003). This, as well as recent bioterrorist events, have emphasized the need for the rapid, accurate and timely monitoring of the quality of drinking water for the presence of pathogens (Rose *et al.*, 1997; Lim *et al.*, 2005). Current pathogen detection methods used in the water quality testing industry are expensive, time-consuming, labour intensive and require highly trained microscopists (Stewart *et al.*, 2005). These methods rely on microscopic examination of samples that are stained with fluorescent antibodies for the presence of the pathogen. The cross-reaction of the antibodies with targets in the sample other than the specific pathogen often gives false positive results. In general, although nucleic acid-based detection systems such as polymerase chain reaction are more sensitive than antibody-based detection systems, they are not highly specific since the background signal (from a multi-component sample) also gets amplified (Lim *et al.*, 2005). By contrast, vibrational spectroscopic techniques such as Raman scattering provide specific molecular information on samples without the need for exogenous labelling. Pathogens can be detected by identifying the unique characteristic vibrational frequencies of the molecular species, even in a complex multi-component mixture (Maquelin *et al.*, 2002; Stewart *et al.*, 2005), allowing for label-free molecularly specific imaging. The Raman effect is, unfortunately, a very weak effect due to the low characteristic cross-sections of spontaneous Raman scattering. This results in a significant disadvantage when using this analytical tool for water testing, as Raman-based approaches will have long data acquisition times. Additionally, the application of conventional Raman spectroscopy can be disadvantageously affected by background fluorescence, which often limits the sensitivity of detection.

Coherent anti-Stokes Raman scattering (CARS) is an approach to enhance the Raman scattered light by means of coherent nonlinear optical excitation of molecular vibrational levels (Rodrigues *et al.*, 2006; Evans & Xie, 2008). CARS microscopy has been demonstrated as a powerful tool for label-free, non-invasive, chemical imaging of biological and material systems. This technique offers many advantages including (i) chemical contrast based on Raman vibrational

‡Current Address: Harvard Medical School and Wellman Center for Photomedicine, 40 Blossom St., BAR 722, Boston, Massachusetts 02114, U.S.A.

Correspondence to: S. Murugkar. Tel: (613) 562 5800 X 2168; fax: (613) 562 5664; e-mail: murugkar@site.uottawa.ca

frequencies, (ii) high sensitivity and rapid detection due to the coherent nature of the CARS process and (iii) sub-wavelength lateral spatial resolution. CARS is a nonlinear optical process that requires two laser frequencies called 'pump' (ω_P) and 'Stokes' (ω_S). When the frequency difference between the pump and Stokes frequencies, $\omega_P - \omega_S$, is tuned into a molecular vibrational frequency in the specimen, a strong blue-shifted signal is generated at the anti-Stokes frequency of $\omega_{AS} = 2\omega_P - \omega_S$. There also exists a non-resonant electronic contribution to the CARS signal that is independent of Raman shift and is often the contrast limiting factor in CARS microscopy. Although CARS microscopy and spectroscopy has been applied to detection of live bacterial cells in laboratory conditions (Zumbusch *et al.*, 1999; Petrov *et al.*, 2005), it has been largely unknown in the water testing industry.

In this paper, we demonstrate CARS microscopy for the rapid imaging of a waterborne pathogen, the protozoan parasite, cryptosporidium parvum, which represents a major threat to human health (Rose *et al.*, 1997; Edge *et al.*, 2003; Lim *et al.*, 2005). Cryptosporidium occurs in contaminated water sources in the form of an oocyst that typically encloses four infection-causing sporozoites inside. The thick oocyst wall is resistant to most chemical water disinfection treatments and ingestion of just a few cryptosporidium oocysts can cause acute diarrhoea in humans. The disease, cryptosporidiosis, can have fatal consequences especially in individuals with weakened immune system, since there is no effective drug therapy to treat cryptosporidial infections. The standard method followed for collecting, identifying and quantifying Cryptosporidia uses immunomagnetic techniques to separate Cryptosporidium oocysts from other components in the collected water, and immunofluorescent staining to assay the oocysts (U.S. Environmental Protection Agency, 1999). This labour-intensive testing procedure takes up to few days to complete. In this paper, we present chemically selective images of cryptosporidium acquired in just a few seconds using CARS microscopy, and illustrate its potential for the rapid identification of cryptosporidium at the single oocyst level. We discuss the applicability of such a technique in a near-real time automated water testing system.

Experimental details

Light source

A schematic of the light source for producing the pump and Stokes beams, is shown in Fig. 1(a). This system was based on two synchronized Ti:sapphire lasers (Tsunami, Spectra-Physics/ Newport, Mountain View, CA, U.S.A.). The output from the two lasers consisted of 3-ps duration optical pulse trains at a repetition rate of 80 MHz. The two lasers were synchronized in a Master/Slave configuration (Spectra Physics, Lock-to-Clok) resulting in a timing jitter of ~0.5 ps. The pump beam was tunable from 700 to 840 nm and the

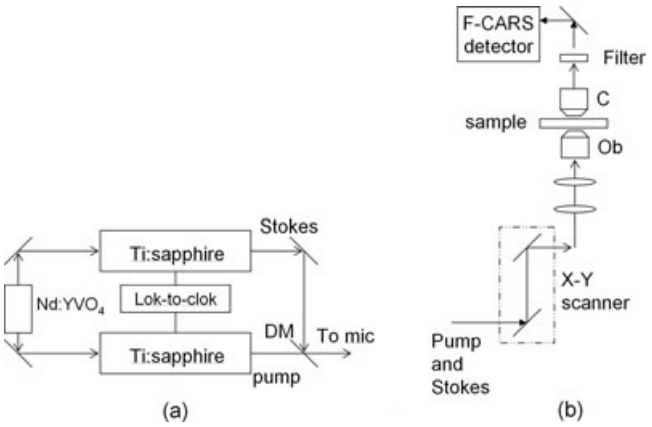

Fig. 1. Schematic of the coherent anti-Stokes Raman scattering (CARS) light source and microscope setup. Nd:YVO4: 1064 & 532 nm laser; DM: dichroic mirror; Ob: 1.2 NA water 60× objective lens; C: 0.55 NA air condenser (a) Light source employing two synchronized Ti:sapphire lasers (b) Laser scanning microscope modified for detecting forward CARS (F-CARS) signal.

Stokes beam from 780 to 900 nm, each with a maximum output power of ~1 W. The optical power at the sample was ~24 mW for the pump beam and ~28 mW for the Stokes beam, respectively.

Microscope

The divergences of the pump and Stokes beams were independently controlled by a telescope in each beam path. An electronic delay control was employed to temporally overlap the two pulse trains. The collinearly overlapped pump and Stokes beams were directed to a laser-scanning microscope (Olympus FV300/IX71, Center Valley, PA, USA) that was modified for CARS microscopy (Fig. 1b). A pair of galvanometer mirrors in the microscope controlled the scanning of the two beams on the sample surface. The pump and Stokes laser beams were focused onto the sample using a water immersion objective lens (UPlanApo IR, 60×, Olympus America, Inc.) with a numerical aperture (NA) of 1.2. The forward CARS signal was collected with an air condenser lens (NA = 0.55) and detected by a photomultiplier tube (R3896, Hamamatsu, Bridgewater, NJ, USA) after passing through a set of bandpass filters (Coherent Ealing, Rocklin, CA, USA).

Samples

Samples of live (viable) Cryptosporidium parvum (C. parvum) oocysts originating from experimentally infected calves (Iowa isolate) were obtained from Waterborne, Inc. (New Orleans, LA, U.S.A.). The oocysts were suspended in a solution of phosphate-buffered saline with antibiotics and a non-ionic surfactant and emulsifier Tween® 20. Due to the hazardous nature of the sample, all sample preparations and imaging experiments were performed in a biosafety level

2 accredited laboratory environment. Several drops of the phosphate-buffered saline solution containing the C. parvum oocysts were placed on top of a microscope slide and covered with a thin (#1) cover slip.

Results

CARS imaging at 2845 cm^{-1} of lipid density in C. parvum oocyst

Raman spectroscopy studies of cryptosporidium reported earlier (Stewart *et al.*, 2005) revealed a strong Raman scattering intensity at ~2850 cm^{-1} corresponding to the CH_2 symmetric stretching mode. For the initial CARS microscopy investigations, the frequency difference between the pump and Stokes beams was set to match the aliphatic CH_2 symmetric stretching vibration of lipids at 2845 cm^{-1}. The wavelengths of the pump and Stokes beams were 716.8 and 900.4 nm, respectively.

Figure 2(a) shows a single live C. parvum oocyst imaged using DIC mode at the wavelength of 816.9 nm. A detailed structural analysis of C. parvum oocysts using light and electron microscopy was reported recently (Petry, 2004). C. parvum oocysts contain four tightly packed sporozoites and a residual body. The residual body is a membrane-bounded structure containing lipid, polysaccharide/amylopectin and protein/amino acids as a storage source of metabolites for the sporozoites (Harris *et al.*, 2004). The CARS image at 2845 cm^{-1} of another live oocyst obtained in the forward direction (F-CARS) is shown in Fig. 2(b), whereas Fig. 2(c) shows the same oocyst imaged at a non-resonant frequency shift of 2710 cm^{-1}. It is evident that when the frequency difference of the excitation beams is tuned to be off-resonance to 2710 cm^{-1}, the contrast in the CARS image disappears and only a weak non-resonant signal remains. This arises from electronic contribution to the third order non-linear susceptibility and is independent of the Raman shift (Rodrigues *et al.*, 2006; Evans & Xie, 2008). This non-resonant CARS background has been subtracted from the image in Fig. 2(b) and the resulting image is displayed in Fig. 2(d). The observation of the bright spherical 1-μm structure corresponding to a high lipid density is consistent with the presence of the lipid vacuole inside the residual body, as identified by electron microscopy (Petry, 2004). Another oocyst imaged at 2845 cm^{-1} (Fig. 2e) shows the same image feature as in Fig. 2(d). This feature is highly reproducible and was repeatedly observed in all CARS images of C. Parvum oocysts at the lipid band. The surrounding region of ~5 μm in diameter, which corresponds to the residual body and sporozoites, contributes a weaker lipid CARS signal. The intensity profile along a line drawn across the image in Fig. 2(e) at 2845 cm^{-1} is shown in Fig. 2(f). It is characterized by a strong peak of about 1 μm width on a pedestal of about 5 μm width. When the incident light pulses are focused at different vertical positions in the oocyst, the dominating CARS signal from the lipid vacuole disappears and only the weaker CARS lipid signal from the sporozoites is visible. This can be visualized in Fig. 3(a), which shows a depth stack obtained by focusing from top to bottom in steps of 0.25 μm of a single C. parvum oocyst at 2845 cm^{-1}.

F-CARS images at 2845 cm^{-1} of a different protozoan pathogen, Giardia lamblia, were taken to demonstrate that the characteristic pattern, size and shape in the CARS image of the lipid distribution in a cryptosporidium oocyst is readily discernible from a different protozoa. A sample comprising non-viable (dead) cysts of Giardia lamblia dried on top of microscope well slides was obtained from GAP EnviroMicrobial

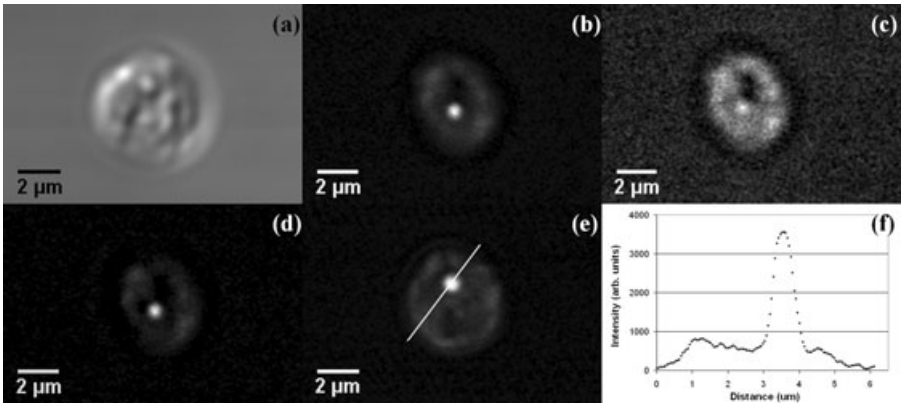

Fig. 2. (a) DIC microscopy image of live C. parvum oocyst (b) F-CARS image of a different live C. parvum oocyst at 2845 cm^{-1}; pump and Stokes beams were 716.8 nm and 900.4 nm, respectively. Image is averaged over two frames (512 × 512 pixels) corresponding to an area of ~125 × 125 μm. The spatial resolution is ~0.2 μm and the acquisition time for this image was ~2 s. (c) Non-resonant coherent anti-Stokes Raman scattering (CARS) signal obtained from the oocyst in (b) at a frequency shift of 2710 cm^{-1}. (d) F-CARS image of the oocyst in (b) after subtraction of the non-resonant background (c). (e) F-CARS image of the lipid distribution inside yet another C. parvum oocyst showing the same image feature as in (b). (f) The intensity profile along a line drawn across the image in Fig 2e at 2845 cm^{-1}.

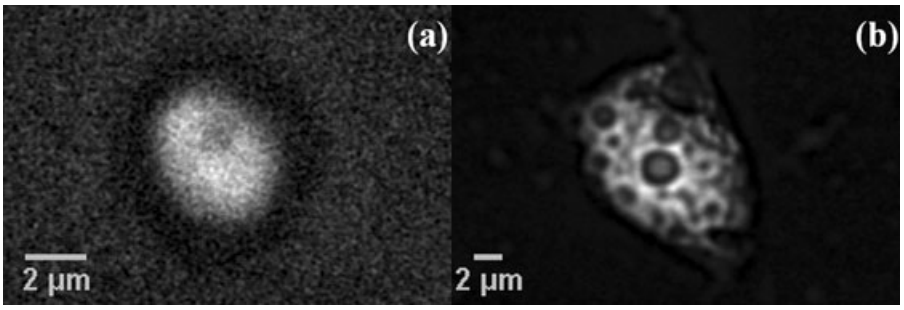

Fig. 3. (a) 3-dimensional movie obtained by focusing from top (frame shown) to bottom in different planes in steps of 0.25 μm inside a C. parvum oocyst. (b) F-CARS image of a non-viable cyst of the protozoan pathogen, Giardia Lamblia at 2845 cm^{-1}.

Services (London, ON, Canada). The CARS image of a single cyst of Giardia lamblia with a characteristic size of about 10–15 μm is displayed in Fig. 3(b). The shape and pattern of the image feature in Fig. 3(b) indicates that the lipid distribution in a Giardia cyst is very different compared to that in the C. parvum oocyst. The size of ~14 μm of the Giardia cyst and the observed structure is consistent with reports in literature (de Souza *et al.*, 2004).

Chemical selectivity in CARS images

The chemically selective nature of CARS microscopy can be advantageously used for mapping the distribution of the protein density inside the C. parvum oocyst. This was done by tuning the frequency difference between the pump and Stokes to match the vibrational frequency at 1650 cm^{-1} corresponding to the amide I molecular vibrations of proteins inside the oocyst. The pump and Stokes wavelengths were at 740.6 and 843.7 nm, respectively. The F-CARS image from live C. parvum oocyst, obtained by tuning into the 1650 cm^{-1} band, is displayed in Fig. 4(a). There is a significant contribution to the CARS signal arising from the residual body. The chemically specific signal at the amide I vibrational band of protein, reveals the presence of high protein density inside the residual body. This result matches the earlier findings of Harris *et al.* who studied thin sections of residual bodies

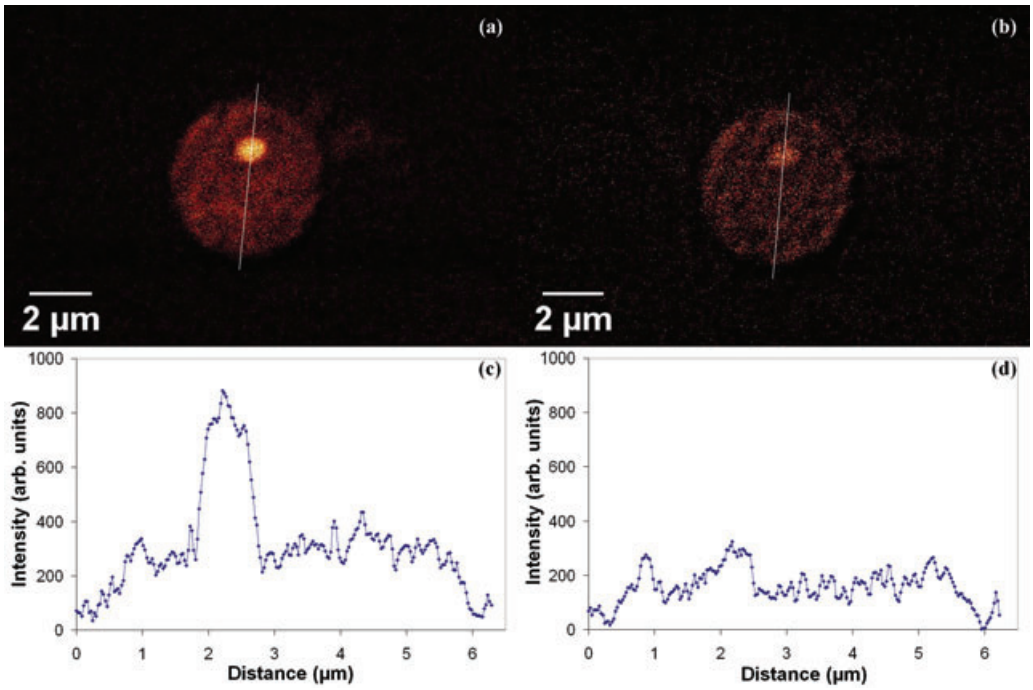

Fig. 4. (a) coherent anti-Stokes Raman scattering (CARS) image of a live C. parvum oocyst at a Raman shift of 1650 cm^{-1} corresponding to the amide I vibrational band characteristic of protein taken in 2s. (b) CARS image of the non-resonant contribution at the Raman shift of 1700 cm^{-1}, also obtained with a 2s integration time. (c) and (d) Intensity profile along a line drawn across the CARS image in (a) and (b), respectively, showing peak intensity in (c) arising from the residual body and remaining non-resonant background in (d).

inside C. parvum oocysts using electron microscopy. They reported that the membrane-enclosed residual body contains a crystalline protein inclusion and numerous amylopectin granules (Harris *et al.*, 2004), which give rise to the large observed amide I CARS vibrational signal.

When the frequency difference between the pump and Stokes beams is tuned off-resonance to 1700 cm^{-1}, this vibrational contrast vanishes as seen in Fig. 4(b). This fact is emphasized in the intensity profiles along a line drawn across the image as shown in Fig. 4(c) and (d). It is evident that only the non-resonant CARS background remains at the Raman shift of 1700 cm^{-1}. Note that the CARS signal is proportional to the square of the concentration of the molecular species inside the focal volume of interaction (Rodrigues *et al.*, 2006; Evans & Xie, 2008). Since the protein and lipid molecules are concentrated inside the same physical space of the residual body, the spatial co-localization of these two signals further supports the assignment of the CH_2 and amide I bands to the features observed in previous electron microscopy studies (Petry, 2004). These co-localized signals may be used as an additional test to identity C. parvum oocysts using CARS microscopy.

CARS imaging of C. parvum oocyst in presence of trapping medium

When a water sample is tested in a water quality testing facility, a large volume (~10–50 L) of water is flown through a filter medium (~1 inch in diameter) made up of a membrane and/or a chemical trapping medium such as chemically treated diatomaceous earth.

An experiment was conducted to demonstrate the feasibility of detecting a cryptosporidium oocyst using CARS microscopy in the presence of a trapping medium. For this purpose, a sample of a chemical trapping medium was obtained from EcoVu Analytics (Ottawa, Ontario, Canada). A small amount of this trapping medium was mixed with water and the slurry was placed on a microscope glass slide. A drop of phosphate-buffered saline solution containing live cryptosporidium parvum oocysts was added to this mixture. This sample was covered with a thin glass cover slip and imaged in the forward direction. One of the resulting CARS images, taken at 2845 cm^{-1}, is shown in Fig. 5. An image feature having the characteristic pattern, shape and size of an individual cryptosporidium oocyst is clearly discernible in the centre of the image. This image feature visualizes the same lipid density pattern consisting of the 1 μm bright spot in the 5 μm circular area corresponding to the cryptosporidium parvum oocyst. A weaker non-resonant CARS signal, which is not related to the lipid molecular vibrations and arises mainly due to electronic contributions from the surrounding trapping medium, is also seen in the CARS image of Fig. 5. A number of techniques have been developed to suppress this non-resonant CARS background signal. In particular, frequency-modulation CARS (FM-CARS) microscopy (Ganikhanov *et al.*, 2006) is especially promising. In FM-CARS, the non-resonant background is suppressed by rapidly toggling the Raman shift on and off a CARS resonance, thereby isolating only the resonant CARS response. Therefore, even weak CARS signals from a pathogen trapped in the aqueous trapping medium could be successfully identified using CARS imaging. An automated image recognition algorithm (Fernandez-Canque *et al.*, 2006) would be useful to distinguish between various types of pathogens based on the observation of distinct CARS intensity profiles/ patterns at 2845 cm^{-1}.

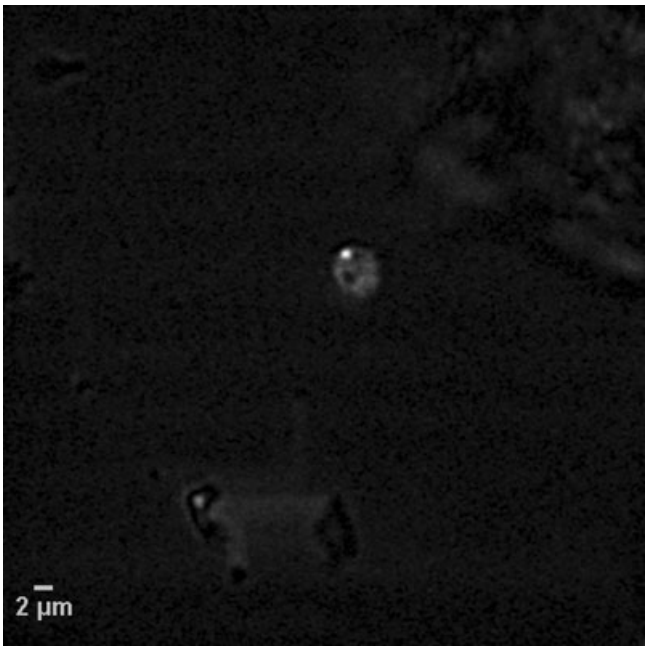

Fig. 5. Coherent anti-Stokes Raman scattering image at 2845 cm^{-1} of a live C. parvum oocyst (centre) in the presence of a chemical trapping medium.

Discussion

Application to water testing

Concentrations of pathogens in drinking water and recreational waters are usually too dilute for direct measurements. Target microorganisms in water samples generally must be concentrated by several orders of magnitude from the water samples using membrane filtration and/or organic trapping medium such as chemically treated diatomaceous earth. The material that has accumulated on the filter is removed, collected and analysed following a lengthy protocol (U.S. Environmental Protection Agency, 1999). One important advantage of CARS microscopy as a detection tool in water quality testing, is that the need for such lengthy sample preparation is eliminated since it relies on the intrinsic vibrational contrast due to various molecular

species present in the pathogen. Due to the coherent nature of the CARS process, the CARS signal is typically several orders of magnitude stronger than other vibrational microscopy techniques such as spontaneous Raman microscopy, thus resulting in very short data acquisition times. A possible implementation of CARS-based imaging for near real-time automated detection of pathogens in water samples is as follows. The volume of water to be tested flows through a trapping medium held at the bottom of a container at a rate of 0.4–4 L min^{-1}. The ideal trapping medium enables concentration of the pathogens in the water sample by 100–10 000 times. The trapping medium would then flow out of this container and into a sampling cell made of transparent quartz glass (with dimensions of about $200 \times 200 \times 100$ μm^3) at a much slower rate (discussed below). CARS images and spectra of the sample cell contents could be taken utilizing a video-rate scanning system for rapid acquisition (Evans *et al.*, 2005). If the time it takes for the trapping medium to fill the sample cell is sufficiently short, this apparatus provides real-time testing of the trapping medium flowing through the sample cell at an average flow rate of about 1.2×10^{-6} cm^3 (cc) per second. Accordingly, it will take about 138 min to test 0.01 cc of the trapping medium, about the amount contained in one drop, corresponding to a water volume of about 1 to 100 cc assuming the pathogen concentration factor provided by the trapping medium is 100 to 10 000. This is in contrast to the time of one week required to test a sample of 100 mL (= 100 cc) to be analysed for *E. coli* bacteria by means of a visual analysis of a specially prepared sample by a skilled technician (U.S. Environmental Protection Agency 1999).

As shown in this paper, the CARS image of the lipid density in a cryptosporidium oocyst has a characteristic pattern, size and shape. As demonstrated in the results, a depth stack is useful to clearly differentiate between organisms as well as colocalization of the protein density with the lipid density could be an added identifier of C. parvum oocyst. An image recognition algorithm for distinctly identifying cryptosporidium oocysts from other pathogens may be used to implement an automated online water monitoring system.

Once a pathogen is identified to be cryptosporidium, the next important issue to be determined is whether the oocyst is viable or not; that is, whether it is capable of causing infection. For this purpose a CARS spectrum of the pathogen can be collected. Such a spectrum can be readily converted into the corresponding Raman spectrum (Vartianen *et al.*, 2006) for comparison to literature. As reported in an earlier study (Stewart *et al.*, 2005), the ratio of intensities of the Raman peaks at 1000 and 1050 cm^{-1} can be used to distinguish between viable and non-viable C. parvum oocysts.

Conclusions

This proof-of-concept work has demonstrated that CARS microscopy can be used for the rapid chemical imaging of waterborne pathogens such as cryptosporidium parvum oocysts. The chemical selectivity combined and high sensitivity of CARS microscopy can be used to detect C. parvum at the single oocyst level in a few seconds of image acquisition time, without the need for labelling the sample. This is in contrast to the many days that are required to detect waterborne pathogens following the currently adopted techniques in water testing laboratories. Our results demonstrate the potential of CARS microscopy and spectroscopy in a near-real time, automated detection system for C. parvum oocysts.

Acknowledgements

We would like to thank Daryl Patterson, Miranda Rowntree, and Garry Palmateer of Gap EnviroMicrobial Services, London, Ontario, Canada for their help in providing the initial samples of non-viable C. parvum oocysts and Giardia Lamblia cysts. We are grateful to Ray Novokowsky of EcoVu Analytics, Ottawa, Ontario, Canada for the samples consisting of the chemical trapping medium. S.M. acknowledges the Ontario Center for Excellence (OCE) travel award (2007). Funding for the CARS microscopy development was provided by the NIH Director's Pioneer Award to X.S.X.

References

de Souza, W., Lanfredi-Rangel, A. & Campanati, L. (2004) Contribution of microscopy to a better knowledge of the biology of Giardia lamblia. *Microsc. Microanal.* **10**, 513–527.

Edge, T., Byrne, J.M., Johnson, R., Robertson, W. & Stevenson, R. (2003) Waterborne pathogens, publication of National Water Research Institute (NWRI), Environment Canada, Burlington, Ontario, Canada. http://www.nwri.ca/threatsfull/ch1-1-e.html. Last accessed date: 13/08/08.

Evans, C.L. & Xie, X.S. (2008) Coherent anti-Stokes Raman scattering microscopy: chemically selective imaging for biology and medicine. *Annu. Rev. Anal. Chem.* **1**, 883–909.

Evans, C.L., Potma, E.O., Puoris'haag, M., Côté, D., Lin, C.P. & Xie, S. (2005) Chemical imaging of tissue in vivo with video-rate coherent anti-Stokes Raman scattering microscopy. *Proc. Natl. Acad. Sci. USA* **102**, 16807–16812.

Fernandez-Canque, H.L., Beggs, B., Smith, E., Boutaleb, T., Smith, H.V. & Hintea, S. (2006) Micro-organisms detection in drinking water using image processing. 6th International IEEE EMBS Special Topic Conference on Information Technology Applications in Biomedicine (ITAB) Conference, Ioannina–Epirus, Greece, October 26–28. http://medlab.cs.uoi.gr/itab2006/proceedings/Medical%20Imaging/25.pdf. Last accessed date: 13/08/08.

Ganikhanov, F., Evans, C.L., Saar, B.G. & Xie, X.S. (2006) High sensitivity vibrational imaging with frequency modulation coherent anti-Stokes Raman scattering (FM CARS) microscopy. *Opt. Lett.* **31**, 1872–1874.

Harris, J.R., Adrian, M. & Petry, F. (2004) Amylopectin: a major component of the residual body in Cryptosporidium parvum oocysts. *Parasitology* **128**, 269–282.

Lim, D.V., Simpson, J.M., Kearns, E.A. & Kramer, M.F. (2005) Current and developing technologies for monitoring agents of bioterrorism and biowarfare. *Clin. Microbiol. Rev.* **18**, 583–607.

Maquelin, K., Kirschner, C., Choo-Smith, L.-P. *et al.* (2002) Identification of medically relevant microorganisms by vibrational spectroscopy. *J. Microbiol. Methods* **51**, 255–271.

Petrov, G.I., Yakovlev, V.V., Sokolov, A.V. & Scully, M.O. (2005) Detection of bacillus subtilis spores in water by means of broadband coherent anti-Stokes Raman spectroscopy. *Opt. Express* **13**, 9537–9542.

Petry, F. (2004) Structural analysis of Cryptosporidium parvum. *Microsc. Microanal.* **10**, 586–601.

Rodriguez, L.G., Lockett, S.J. & Holtom, G.R. (2006) Coherent anti-Stokes Raman scattering microscopy: a biological review. *Cytometry A* **69A**, 779–791.

Rose, J.B., Lisle, J.T. & LeChevallier, M. (1997) *Waterborne Cryptosporidiosis: Incidence, Outbreaks and Treatment Strategies, in Cryptosporidium and Cryptosporidiosis* (ed. by R. Fayer), pp. 93–109. CRC Press, Boca Raton, Florida.

Stewart, S., McClelland, L. & Maier, J. (2005) A fast method for detecting Cryptosporidium parvum oocysts in real world samples. *Proc. SPIE* **5692**, 341–350.

U.S. Environmental Protection Agency (1999) *Method 1623: Cryptosporidium and Giardia in water by filtration /IMS/FA EPA-821-R-99-006*. U.S. Environmental Protection Agency, Office of Water, Washington, DC.

Vartianen, E.M., Rinia, H.A., Müller, M. & Bonn, M. (2006) Direct extraction of Raman line-shapes from congested CARS spectra. *Opt. Express* **14**, 3622–3630.

Zumbusch, A., Holtom, G.R. & Xie, X.S. (1999) Three-Dimensional vibrational imaging by coherent anti-Stokes Raman scattering. *Phys. Rev. Lett.* **82**, 4142–4145.

